North Dakota Water Resources

Implementing Earth Observations Data to Assess Water Quality of Inland Lakes in North Dakota

Summer 2025 | Massachusetts – Boston
June 18th, 2025

Authors: Geetika Godavarthy (Analytical Mechanics Associates), Milena Perez-Gerus (Analytical Mechanics Associates), Logan Rajah (Analytical Mechanics Associates), Mrinalee Reddy (Analytical Mechanics Associates)

Abstract: North Dakota's lakes and reservoirs are popular sites for recreation, wildlife, and water supply. Activities on these lakes peak in the warm summer months, which coincide with changes in water quality as indicated by harmful algal blooms (HABs), high turbidity, and low water clarity. However, funding and staffing constraints across the state create challenges in assessing spatiotemporal changes in lake water quality using in situ data sources. We partnered with the North Dakota Department of Environmental Quality (ND DEQ) Division of Water Quality, who's current HAB monitoring relies on in situ sampling following public reports of blooms. We addressed these limitations using LakeSense – a new Python-based processing pipeline for the automated retrieval of lake water quality indicators from optical remote sensing data, including Sentinel-2 Multispectral Instrument (MSI), Landsat 8 Operational Land Imager (OLI), and Landsat 9 OLI-2. We constructed time series and maps of yearly and monthly climatologies of surface chlorophyll-a, turbidity, and Secchi depth from 2015 to 2025, between May and October, for five lakes across North Dakota. The results showcased seasonal patterns across all study lakes. Chlorophyll-a peaks aligned with in situ HABs sampling events, indicating that remotely sensed LakeSense values were viable indicators to study HABs. Limitations included reduced data availability for smaller or narrower lakes due to increased adjacency effect errors and limited in situ measurements for validation. Incorporating these outputs into decision-making can help ND DEQ target sampling during high-risk periods and improve long-term monitoring of HAB trends across North Dakota's lakes.

Key Terms: Sentinel-2, Landsat 8, Landsat 9, Harmful Algal Blooms, chlorophyll-a, turbidity, Secchi depth, inland aquatic remote sensing

Advisors: Dr. Cédric G. Fichot (Boston University), Sachini Ranasinghe (Boston University)

Lead: Madi Arndt (Massachusetts – Boston)

1. Introduction

1.1 Background Information

North Dakota, located in the Northern Great Plains region, is home to over 295 public lakes and reservoirs ranging from large, terminal saline lakes to numerous smaller reservoirs (North Dakota Department of Health, 2019). Many of these lakes are classified as eutrophic based on lake water quality indicators (LWQI), such as low dissolved oxygen, excessive nutrient loading, and siltation. Eutrophic lakes are typically unfit to serve as sources of drinking water, support aquatic wildlife habitats, or provide resources for recreational, agricultural, and industrial use. Erosion, runoff from cropland, livestock operations, and hydrologic modifications have contributed to decreased water quality in lakes (North Dakota Department of Health, 2019). Additionally, rising water temperatures and precipitation have exacerbated issues related to nutrient inputs and sedimentation within these lakes, leading to a greater incidence of harmful algal blooms (HABs) in recent years (United States Environmental Protection Agency, 2016). This highlights the need to increase frequent and consistent water quality monitoring efforts across the region.

Satellite-based Earth observation data allows for large-scale, spatiotemporally dense analysis of lake water quality, without facing the accessibility or resource constraints that in situ sampling incurs. The spectral signatures of optically active materials in natural waters can be used to assess key LWQIs and ecological trends (Sun et al., 2024). Researchers have used a range of empirical, analytical, semi-analytical, and machine learning algorithms in tandem with in situ data in previous studies to derive the water quality of both inland and coastal waters (Chen et al., 2025). However, there are currently no standardized products for aquatic reflectance from higher spatial resolution sensors such as Landsat 8, Landsat 9, or Sentinel-2. Specialized atmospheric corrections are required to mitigate the effects of cloud cover, aerosols, and adjacency from reflective land surfaces.

To address these limitations, this study utilized Earth observation data obtained from LakeSense, an unreleased automated data pipeline that acquires satellite imagery from Sentinel 2A-B MultiSpectral Instrument (MSI), Landsat 8 Operational Land Imager (OLI), and Landsat 9 OLI-2 (Nolte et al., 2025). The pipeline increases the volume and frequency of data by combining observations from the instruments and automates lengthy atmospheric correction processes for the retrieval of water reflectance through Level-2 masks and Quality Water Index Polynomial (QWIP) filtering to exclude low-quality retrievals. Specialized atmospheric corrections are necessary to retrieve LWQI's such as chlorophyll-a, turbidity, and Secchi depth (Castagna & Vanhellemont, 2025; Pan & Bélanger, 2025). Chlorophyll-a concentration is primarily used to monitor eutrophication and HABs, with seasonal peaks observed in the summer (Sun et al., 2024; Karimi et al., 2024). Turbidity measures particle suspension and is used to indicate high sediment influxes (Mishra et al, 2024; Kulkarni, 2011). The Secchi disk depth measures water transparency and is used as an indicator of ecosystem productivity and eutrophication (Jia et al., 2022).

1.2 Project Partner + Objectives

We partnered with the North Dakota Department of Environmental Quality's (ND DEQ) Division of Water Quality to identify changes in water quality for five North Dakota lakes using LakeSense. The partner's current monitoring efforts include in situ sampling efforts following public HAB reports, in addition to long-term initiatives that monitor chlorophyll-a, Secchi depth, and turbidity (WMP Factsheet). However, ND DEQ faces obstacles in collecting consistent, routine samples due to limited staffing, resources, and funding. This project can assist the partners with refining their water management protocols by increasing the availability of water quality data across all lakes of interest. It serves as a feasibility study to demonstrate the potential of LakeSense to generate long-term water-quality time series that can support ND DEQ's decision-making processes, such as refining water management protocols and providing public communication on water quality trends.

To quantify and visualize changes in water quality, we applied Earth observation data obtained through LakeSense to five lakes chosen by the project partner: Devils Lake, Lake Ashtabula, Jamestown Reservoir, Bowman-Haley Dam, and Patterson Lake (Figure 1). We produced time series plots and maps of chlorophyll-

a, Secchi depth, and turbidity, from 2015 to 2025. Simultaneously, we aimed to provide our partners with comprehensive long-term data to streamline their LWQI monitoring efforts.

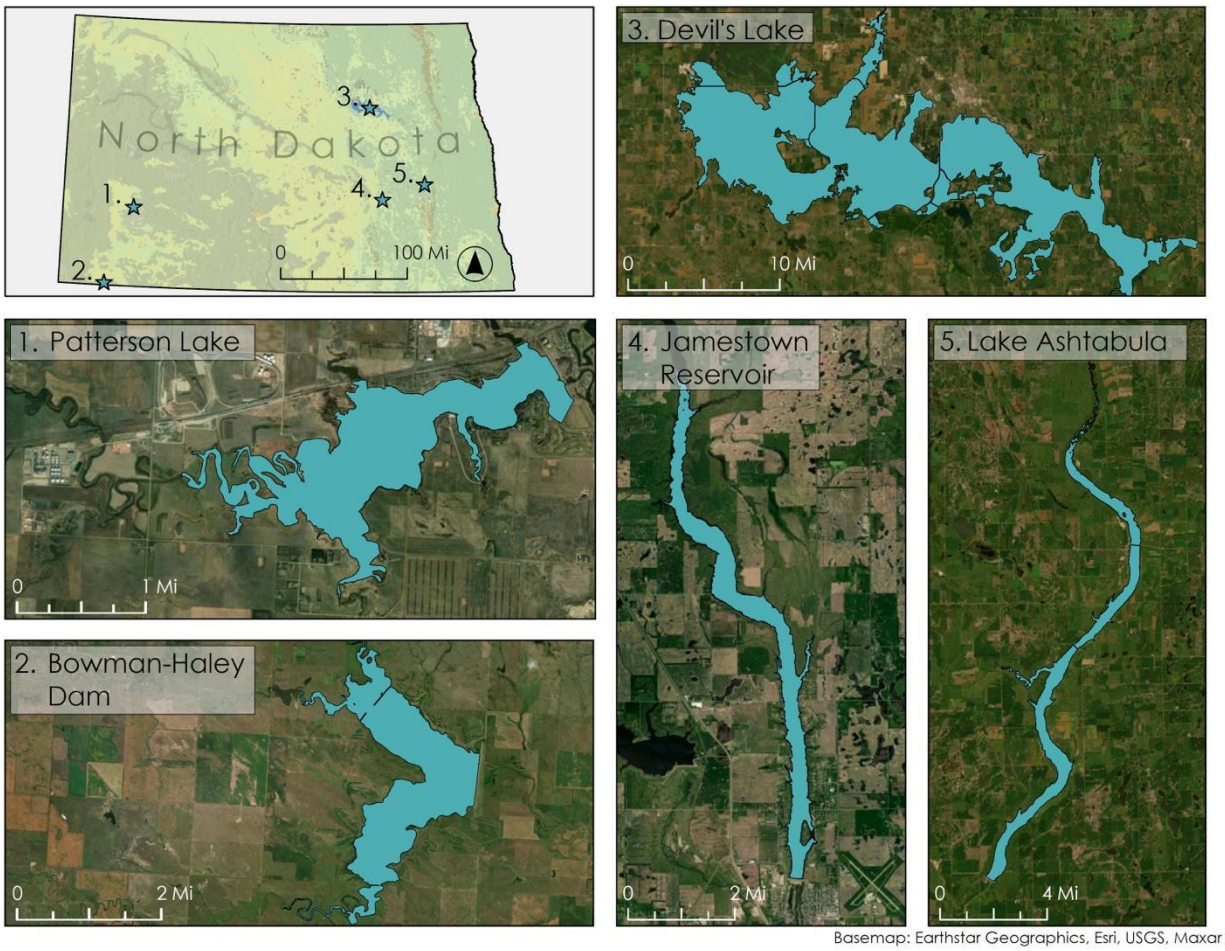

Figure 1. The study area includes the 5 lakes of interest located across North Dakota. Inset scales vary by lake.

2. Methodology

2.1 Data Acquisition

2.1.1 Satellite Data

The LakeSense pipeline first performed satellite image acquisition using the lakes' National Hydrography Dataset Identification number (NHD ID) as the primary input. Based on the NHD ID, we determined which satellite imagery to download by selecting imagery that covered the designated lake areas. We filtered the imagery with a cloud cover threshold of 50%, and a date range of 2013-2023, specifically within the summer months (April to October) to retrieve results with optimal weather conditions and avoid frozen lake conditions. Finally, we extracted the data from Sentinel-2 MSI, Landsat 8 OLI, and Landsat 9 OLI-2 using image downloading queries through their respective APIs in Python. We obtained Sentinel-2 MSI, Level 1 (L1) and Level 2 (L2) products via the Copernicus Data Space Ecosystem (CDSE) data portal. Similarly, for Landsat 8 OLI and Landsat 9 OLI-2, we obtained Collection 2 L1 and L2 products through the U.S. Geological Survey (USGS) EarthExplorer data portal. To facilitate atmospheric correction processing, the LakeSense pipeline automatically downloaded ancillary meteorological metadata from meteorological satellites (MET) to provide necessary parameters such as atmospheric pressure and wind speed for atmospheric corrections.

Table 1. *Earth Observations Datasets Used for Data Acquisition*

Platform and Sensor	Data Product	Acquisition Method
Sentinel-2 MSI	MSI Collection 1 Level-1C TOA Reflectance Product MSI Collection 1 Level-2A BOA Reflectance Product	Copernicus Space Data Ecosystem
Landsat 8 OLI	OLI Collection 2 Level 1 OLI Collection 2 Level 2 Surface Reflectance Product	USGS EarthExplorer
Landsat 9 OLI-2	OLI-2 Collection 2 Level 1 OLI-2 Collection 2 Level 2 Surface Reflectance Product	USGS EarthExplorer

2.1.1 In situ Data

For data validation, we acquired multiple in situ chlorophyll-a and Secchi depth datasets from the ND DEQ Division of Water Quality for lakes in North Dakota between 2013 and 2024. We obtained turbidity measurements from the National Water Quality Monitoring Council's Water Quality Portal (WQP), a publicly available water quality database that integrates data sources from federal and state-level agencies (Table 2). Due to the sparsity of these datasets, we also obtained a log of major HAB events from the ND DEQ Division of Water Quality between 2020 and 2024.

Table 2. *In situ Datasets*

In situ dataset	Date Range	Source
Chlorophyll-a	2015-2025	ND DEQ Division of Water Quality
Secchi Depth	2013-2024	ND DEQ Division of Water Quality
Turbidity	2013-2025	Water Quality Portal
Notable HAB Observations	2020-2024	ND DEQ Division of Water Quality

2.2 Data Processing

2.2.1 R_{rs} retrieval

To derive LWQI, LakeSense retrieved lake-water remote-sensing reflectance (R_{rs}) spectra from the obtained satellite imagery. R_{rs} is defined as the ratio of water-leaving radiance to downwelling irradiance just above the water surface (Pahlevan et al., 2017). To do so, LakeSense applied optimal atmospheric corrections to Level 1 data products. These atmospheric correction algorithms also address challenges specific to inland water remote sensing. A major obstacle to accurate R_{rs} retrieval is the adjacency effect, which refers to excess scattering over the target water body, caused by high reflectance from surrounding bright land surfaces (Castagna & Vanhellemont, 2025; Pan & Bélanger, 2025). In contrast, the Level 2 data products are pre-processed using land-specific algorithms like the Landsat Land Surface Reflectance Code (LaSRC) (Vermote, 2016) and Sentinel Sen2Cor (Main-Knorn et al., 2017). However, these are not optimized for inland aquatic remote sensing. Within LakeSense, the following aquatic atmospheric correction algorithms were applied to Level-1 products: ACOLITE DSF (Castagna & Vanhellemont, 2025), ACOLITE RAdCor (Castagna & Vanhellemont, 2025), ACOLITE Exponential Extrapolation (EXP) (Castagna & Vanhellemont, 2025), POLYMER (Karthick et al., 2024), and Genetic Algorithm for Atmospheric Correction (GAAC) (Pan & Bélanger, 2025). For each chosen lake, we ran all the algorithms and selected the most appropriate correction based on the unique properties of the lake.

2.2.2 LWQI retrieval

To convert R_{rs} into physically quantifiable variables for our analysis, we derived three LWQI (chlorophyll-a, turbidity, and Secchi depth) through LakeSense. LakeSense calculates LWQIs from the atmospherically corrected R_{rs} spectra using various remote sensing water quality algorithms (Table 3). We chose the optimal algorithm for each LWQI for each lake based on preexisting lake conditions.

Table 3. *Remote sensing water quality algorithms*

Chlorophyll-a	**Turbidity**	**Secchi Depth**
OC2 (O'Reilly & Werdell, 2019)	Nechad RED (Nechad et al., 2010)	QAA-RGB (Pitarch & Vanhellemont, 2021)
Gons (Gons, 2002)	Nechad NIR (Nechad et al., 2010)	K_d model (Lee et al., 2013)
Mishra (Mishra & Mishra, 2012)	Novoa Blended (Novoa et al., 2017)	Z_{SD} model (Lee et al., 2015)
Bramich (Bramich et al., 2021)		

2.2.3 Extraction and filtering

Following water quality calculations, we applied flags to the processed values in LakeSense to reduce noise and filter for outliers. Each atmospheric correction has a unique flagging process that identifies and removes unsuitable pixels. To determine which correction to use for each case study lake, we tested and compared multiple flag combinations, ultimately selecting the combination that produced the highest quality data for analysis and visualization.

To analyze the LWQI concentrations, we applied one of four extraction masks based on the shape and size of the lake: a lake with no buffer, a lake with a 60-m buffer, a lake with a 120-m buffer, and the Pole of Inaccessibility (POI). The buffers we applied extended inward from the shoreline of the lake, and we extracted the mean and median value across pixels within the lake as defined by the buffer. These buffers omit shallow water pixels near the lake's boundaries from the LWQI extraction, and we chose the buffer distance based on the size and shape of the lake. We algorithmically determined the POI as the point within a lake that is the furthest possible distance from the shoreline boundaries. To extract LWQI using the POI mask, we used the mean and median values of 9 pixels (3x3) centered on the point. We chose to extract data using POI, a shoreline buffer, or no buffer based on the shape and depth of the lake. For example, we used a 60-m buffer for Jamestown Reservoir due to its long and narrow shape (width ≈ 300 m), whereas we used a 120-m buffer for Devils Lake due to its relatively large area and elliptical shape.

To conduct quality assurance on the data, we further filtered the data using the QWIP score, which analyzes the reliability of lake water reflectance. It evaluates the quality of the data based on the spectral shape of the lake reflectance. The algorithm assigns each pixel a QWIP score, based on which they should be kept or flagged as a potential outlier to be removed. Doing so helps eliminate spectral features related to optically shallow water and previously incorrectly removed reflected values (Dierssen et al., 2022). The QWIP filter removes negative values, which also helped clean the data and calculate the mean and median values.

2.3 Data Analysis

2.3.1 Time series plots and Box plots

To observe changes, trends, and spikes in LWQI values over time for the five case study lakes, we created time series plots for chlorophyll-a, turbidity, and Secchi depth for the entire study period, focusing on summer months between April and October. We tested combinations of atmospheric corrections, flags, LWQI algorithms, and filtering methods to create unique masks for time series analysis. For comparison with in situ data, we added red vertical lines that represent ND DEQ Division of Water Quality logged in situ HAB events between 2020 and 2024. This helped us determine how accurately the remotely sensed LWQI can act as proxies for identifying HABs. To better showcase LWQI trends through a single summer season, we isolated yearly snapshots of each indicator from the overall timeseries of every lake. We chose to focus on

2023 to standardize the analysis across lakes and due to the high number of in situ HAB sampling events in that year. To visualize seasonal changes and summer trends (April to October) across our 7-year study period, we also created box plots of monthly average remotely sensed chlorophyll-a, turbidity, and Secchi depth values. This helped us understand when HABs typically occur.

2.3.2 Time series maps and HAB maps

To further investigate trends in LWQI for each of our study lakes, we generated case study maps of chlorophyll-a, turbidity, and Secchi depth for specific dates where we observed peaks in chlorophyll-a in the yearly timeseries snapshot (2023). We used these maps to visualize areas characterized by poor lake water quality over the summer period and could potentially experience similar conditions in future years. To further visualize areas of high HAB activity, we produced maps of each lake with markers to indicate the locations of in situ sampling conducted by the ND DEQ Division of Water Quality. The markers are colored to indicate the concentration of microcystin sample collected. The in situ measurements are binned into low, moderate and high microcystin concentrations. This enables us to understand where HABs typically occur based on locations HAB reports and in situ sampling recorded between 2020 – 2024.

3. Results

This section focuses on Devils Lake and Patterson Lake. Please see appendix for the remaining results for Jamestown Reservoir, Bowman-Haley Reservoir, and Lake Ashtabula.

3.1 Analysis of Results

3.1.1 Atmospheric Corrections and Algorithm Selection

After comparing atmospheric corrections and water quality algorithms, we selected the Mishra algorithm to estimate chlorophyll-a levels across each lake (Mishra & Mishra, 2012), the Z_{SD} algorithm to estimate Secchi depth (Lee et al., 2015), and the Novoa blended algorithm to estimate turbidity (Novoa et al., 2017). Additionally, ACOLITE DSF was most often applied to retrieve chlorophyll-a, ACOLITE RAdCor for Secchi depth, and a mixture of GAAC-1 and the ACOLITE corrections for turbidity. Table 4 showcases the final LWQI and atmospheric correction (AC) algorithms used in this project for each parameter and lake. The mask column indicates the buffer chosen for each lake.

Table 4. *LWQI and atmospheric correction algorithm combinations applied to satellite images for each lake*

Lake	Mask	Chlorophyll-a	Secchi depth	Turbidity
Devils Lake	120-m	**LWQI:** Mishra **AC:** ACOLITE DSF	**LWQI:** Z_{SD} **AC:** ACOLITE RAdCor	**LWQI:** Novoa blended **AC:** ACOLITE Exponential Extrapolation (EXP)
Lake Ashtabula	60-m	**LWQI:** Mishra **AC:** ACOLITE DSF	**LWQI:** Z_{SD} **AC:** ACOLITE RAdCor	**LWQI:** Novoa blended **AC:** GAAC 1
Patterson Lake	60-m	**LWQI:** Mishra **AC:** ACOLITE DSF	**LWQI:** Z_{SD} **AC:** ACOLITE RAdCor	**LWQI:** Novoa blended **AC:** ACOLITE RAdCor
Bowman-Haley Reservoir	60-m	**LWQI:** Mishra **AC:** ACOLITE RAdCor	**LWQI:** Z_{SD} **AC:** ACOLITE RAdCor	**LWQI:** Novoa blended **AC:** GAAC 1
Jamestown Reservoir	60-m	**LWQI:** Mishra **AC:** ACOLITE DSF	**LWQI:** Z_{SD} **AC:** ACOLITE RAdCor	**LWQI:** Novoa blended **AC:** ACOLITE RAdCor

The Mishra algorithm leverages the use of the red-edge band (700 nm) for chlorophyll-a estimation. This improves the accuracy of estimations even in the presence of dissolved organic matter and other suspended

solids (Mishra & Mishra, 2012). However, the Mishra algorithm uses the red-edge band (700 nm) only available in Sentinel satellites, thus excluding Landsat imagery from our chlorophyll-a analysis. We chose Novoa blended because it utilizes a weighted blending scheme to analyze water quality and then pick either the red or NIR reflectance band for turbidity estimation (Novoa et al., 2017). In clearer waters, the red band influences the algorithm, and in more turbid water, the NIR band influences the algorithm. The Z_{SD} model improves upon previous Secchi depth models by only relying on the diffuse attenuation coefficient (K_d) at the wavelength of maximum transparency, improving Z_{SD} measurements in highly turbid waters (Lee et al., 2015).

3.1.2 Devils Lake Results

Timeseries results from Devils Lake indicated a relationship between the in situ sampling of HABs by the North Dakota DEQ Division of Water Quality and peaks in remotely sensed chlorophyll-a values obtained through LakeSense (Figure 2). This coincided with moderately high turbidity values, which indicates cloudiness due to a high concentration of suspended solids and lower Secchi depth values, implying poor water clarity. Overall, Secchi depth values remained the most consistent over time, fluctuating between 0 and 4 meters, with a few very high spikes in 2016 and 2018. Turbidity values remained relatively consistent as well (0 to 15 FNU), with an additional pattern of regular, repeated spikes at the beginning of each summer season. Finally, chlorophyll-a is more variable, but with consistently higher values later in the season. There are fewer data points here, as the Mishra algorithm used to derive chlorophyll-a utilizes the red-edge band (700 nm) only available in Sentinel satellites, thus excluding Landsat imagery from our analysis. Additionally, these values start from 2018, rather than 2015, due to sparse Sentinel-2 Level-1C data coverage during the first two to three years of launch.

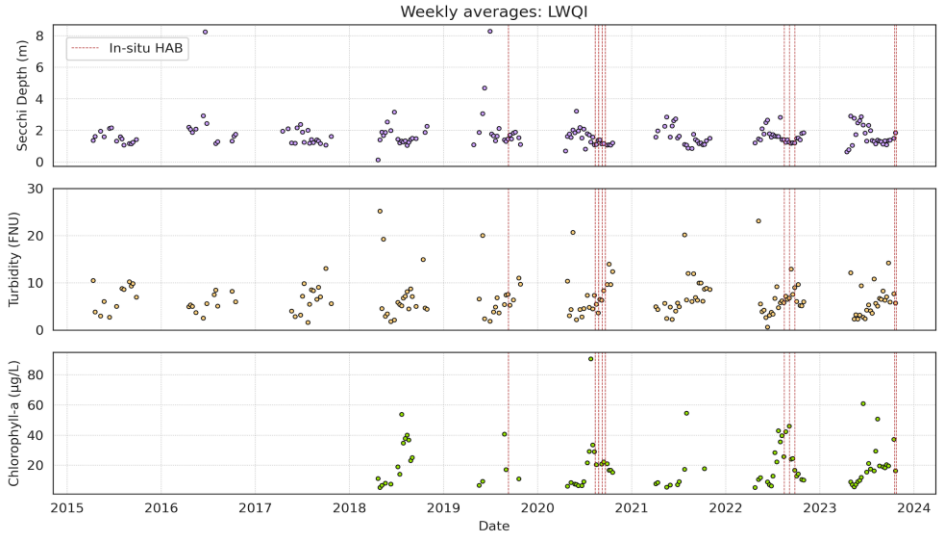

Figure 2. Time series of weekly average LWQI values across Devils Lake. Each time series plot represents monthly average Secchi depth, turbidity, and chlorophyll-a trends from 2015/18 to 2023.

Boxplot results show strong seasonal trends in LWQIs (Figure 3). Chlorophyll-a peaked in the hottest summer months of July and August, coinciding with the lowest dips in Secchi depth concentrations. Turbidity values are moderately high during the same months, with aforementioned peaks in April. This is likely an artifact of frozen lake conditions persisting into April, where there can be increased sediment input from snowmelt runoff.

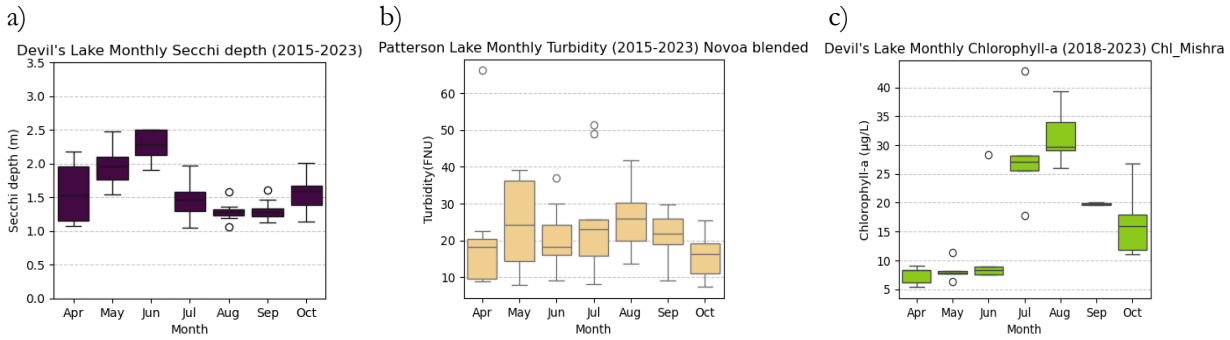

Figure 3. Seasonality boxplots of monthly average Secchi depth (a), turbidity (b), and chlorophyll-a (c) across Devils Lake from 2015/2018 to 2023.

Snapshots from 2023 provide a better representation of LWQI patterns observed during a single summer season (Figure 4). Results indicate a steady decrease in Secchi depth values as the year progresses, while chlorophyll-a values increase once again. Here, the major peaks in June, August, and October are more clearly visible. Turbidity values show large variability from week to week, with occasional spikes. Notably, early June sees high values across all variables, especially chlorophyll-a and turbidity. The three LWQI on the date of this peak (06/17) are mapped in Figure 5 to visualize the incident.

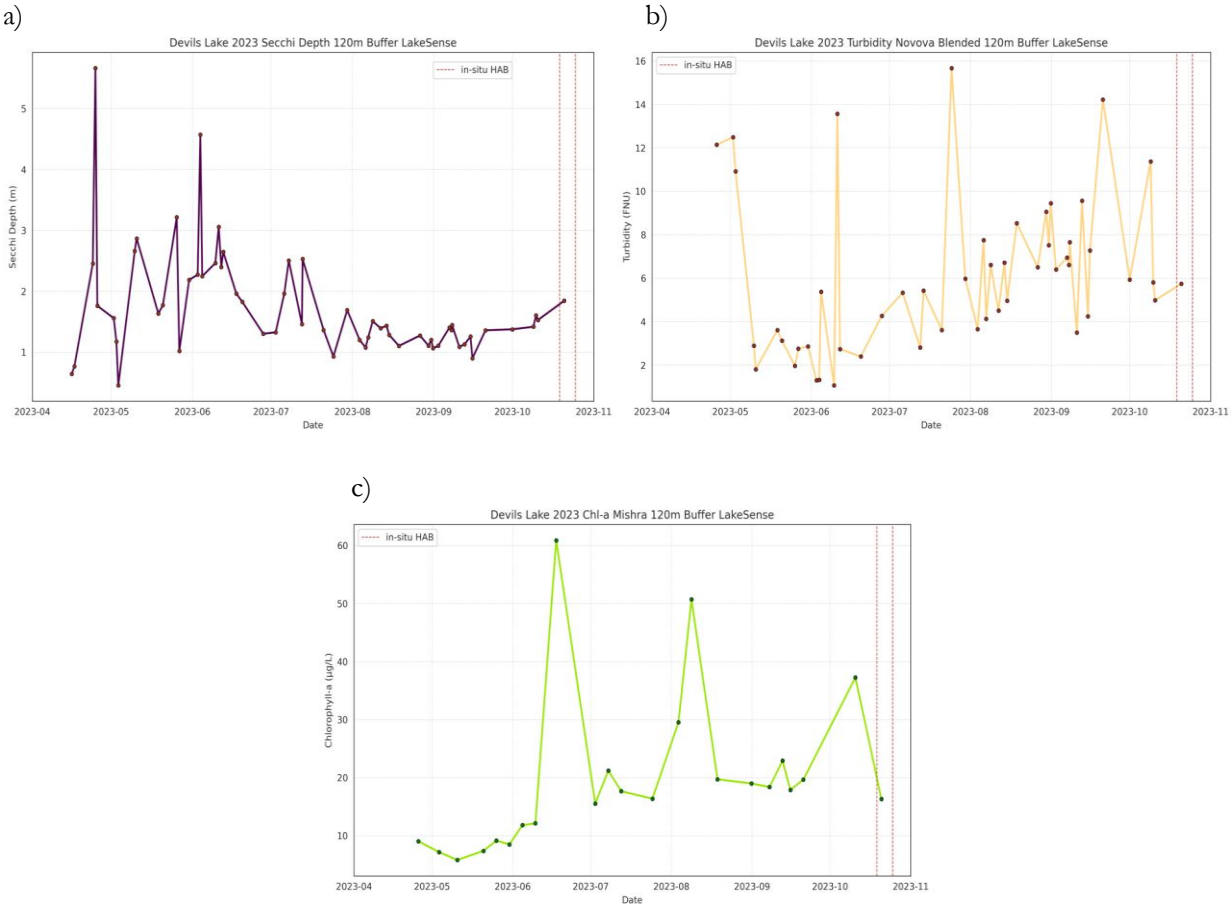

Figure 4. Subset snapshots of weekly average Secchi depth (a), turbidity (b), and chlorophyll-a (c) across Devils Lake from April to November 2023

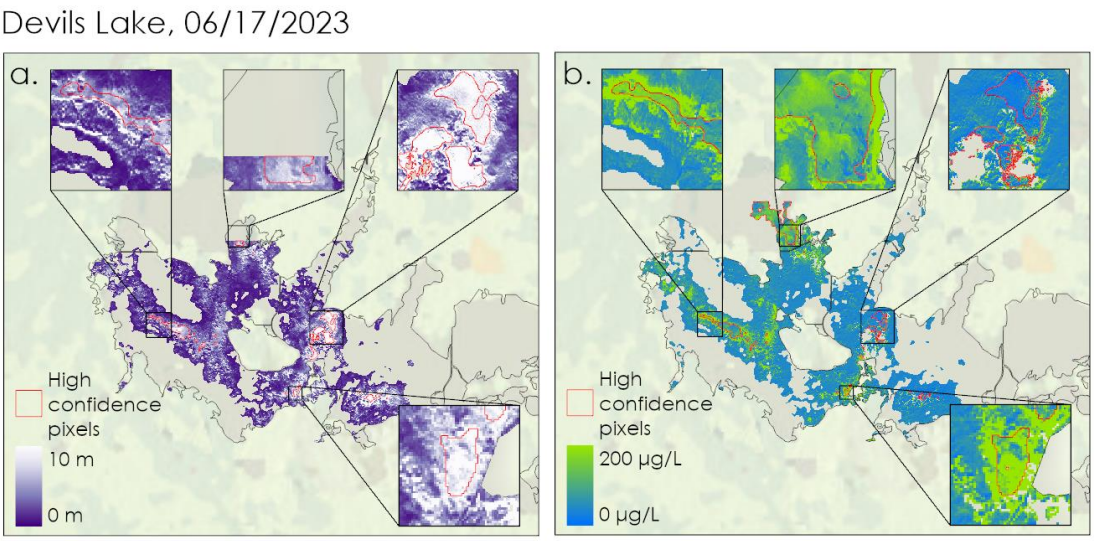

Figure 5. Two-panel map of Secchi depth (a) and chlorophyll-a (b) concentrations in Devils Lake on 17th June 2023. There were insufficient high confidence pixels for the turbidity LWQI for mapping.

The red boundary in Figure 5 indicates the location of the high-confidence pixels that passed all LakeSense flagging procedures. The remaining pixels were also flagged but with lower confidence. For this image, there was a minimal number of pixels with high confidence, as seen in the inset maps. Turbidity for this image on June 17th, 2023, could not be displayed as it did not pass any of the flagging procedures. Within the high confidence pixels, chlorophyll-a and Secchi depth follow inverse trends where chlorophyll-a is high in the same areas in which Secchi depth is low, which could be indicative of HABs.

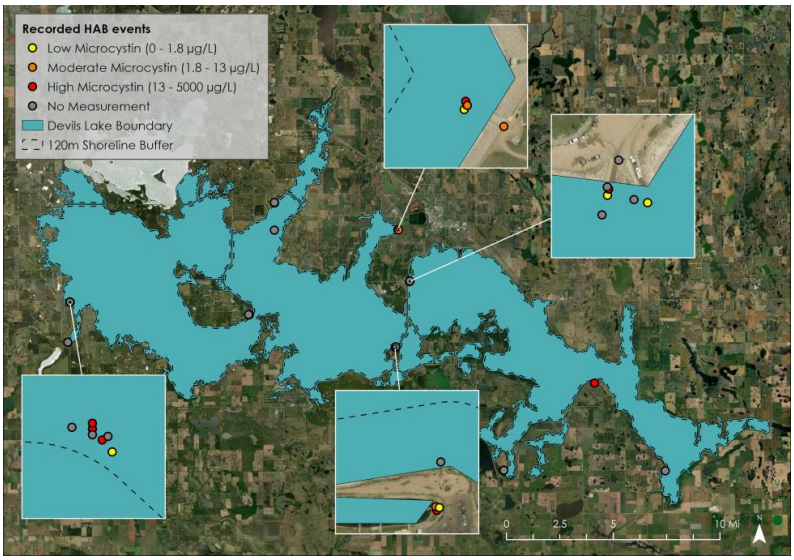

Figure 6. Map of recorded in situ HAB events in Devils Lake (2020-2024)

The map of recorded in situ HAB events displays locations of high HAB activity in Devils Lake, based on ND DEQ sampling efforts. These mostly occur along the shoreline, near docks and boat ramps in the western portion of the lake. In situ sampling was done using the ELISA method Enzyme-Linked Immunosorbent Assay (ELISA) method to obtain microcystin concentration. Due to extreme values >100 µg/L in the dataset, we binned the measurements into quantiles for the purpose of mapping. HAB reports

without a microcystin measurement are also mapped. It should be noted that most sampling points fall outside of the 120-m lake buffer used for LWQI extraction.

3.1.3 Patterson Lake Results

Time series results from Patterson Lake indicate a similar relationship between the in situ sampling of HABs by the North Dakota DEQ Division of Water Quality and peaks in remotely sensed chlorophyll-a values (Figure 7). In this time series, an overall inverse relationship between Secchi depth and turbidity can be observed. Turbidity values show high variability within each year but display a gradual upward trend over the entire study period. The average turbidity rose from ~10 in 2015 to ~20 FNU in 2023. We observed a similar but inverse trend for Secchi depth, where values are gradually decreasing over the study period. This signals an overall trend toward declining water clarity in Patterson Lake. Chlorophyll-a shows similar variability to Devils Lake, except for large peaks in 2021. Finally, as indicated by the vertical red lines, there are far more in situ HAB events recorded for Patterson Lake.

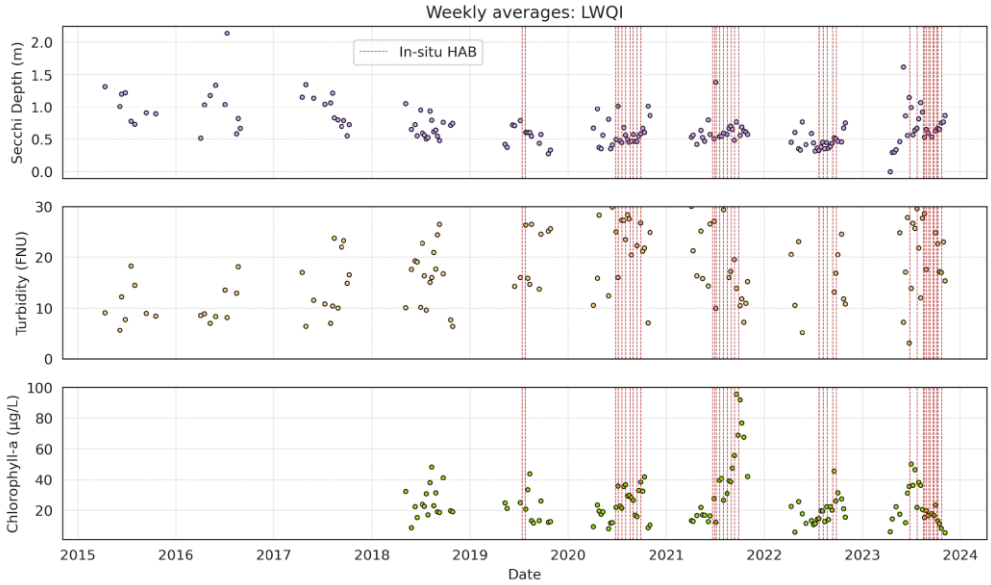

Figure 7. Time series of weekly average LWQI values across Patterson Lake. Each time series plot represents monthly average Secchi depth, turbidity, and chlorophyll-a trends from 2015/2018 to 2023.

Boxplot results for Patterson Lake show moderate seasonal trends in LWQIs (Figure 8). The boxplots for Patterson Lake show weaker peaks as compared to Devils Lake, as there is less variation in values for each parameter. Chlorophyll-a peaks in the hottest summer months of July and August. Secchi depth values do not have much variation throughout the summer, with minor dips in the months of July, August, and September. Turbidity values are moderately high during the months of April and August.

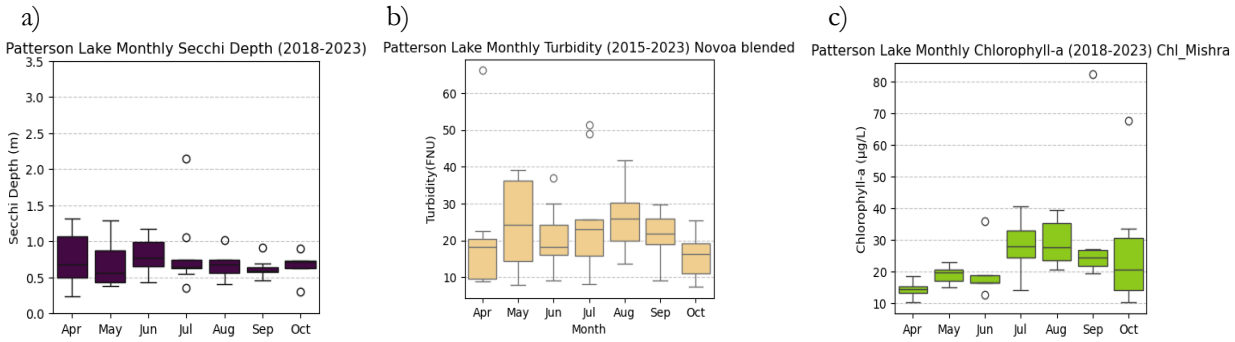

Figure 8. Seasonality boxplots of monthly average Secchi depth (a), turbidity (b), and chlorophyll-a (c) across Patterson Lake from 2015/2018 to 2023

Snapshot results from 2023 show peaks in Secchi depth values in June and July, with values significantly decreasing after August. Chlorophyll-a concentrations peak in July, not aligning with peaks in turbidity, which occur in May and August. Turbidity values again show high variability from week to week, with sharp spikes and dips. Notably, late June saw high values in chlorophyll-a and Secchi depth, which coincides with a recorded in situ HAB event. The three LWQI on the date of this peak (06/30/2023) are mapped in Figure 9 to visualize the incident.

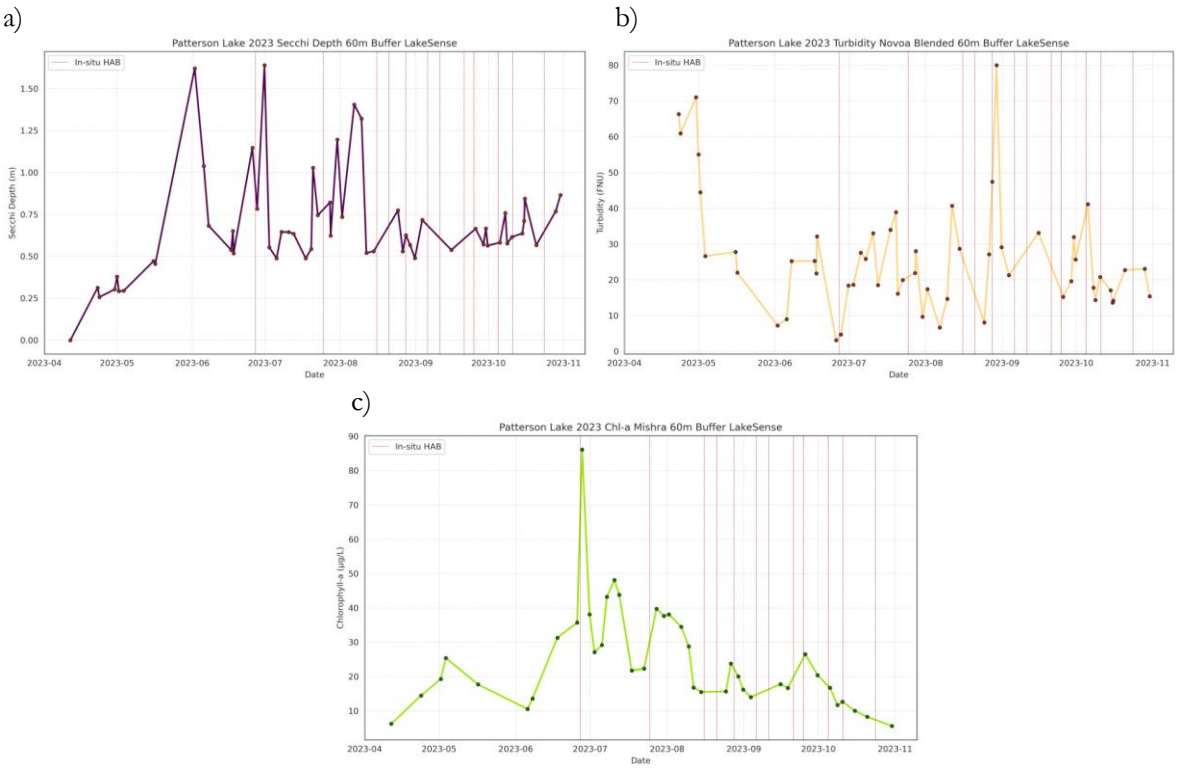

Figure 9. 2023 snapshots of monthly average Secchi depth (a), turbidity (b), and chlorophyll-a (c) across Patterson Lake from April to November 2023

All pixels shown in Figure 10 passed the flagging filters in LakeSense (indicated by the red boundary) and allow for a high-confidence interpretation of the LWQI distribution on the chosen date. Patterson's Lake experienced high chlorophyll-a concentration in the western portion of the lake on June 30th, 2023, as indicated by the strong green swirls (Figure 10c). The southern arm region of the lake showcases the highest

turbidity values at ~50 FNU. Secchi depth values are lower in the same arm, as seen by the dark purple pixels, further showcasing the inverse relationship mentioned above. These concentrations are the highest in the eastern portion of the lake, indicating the poorest water clarity in that area.

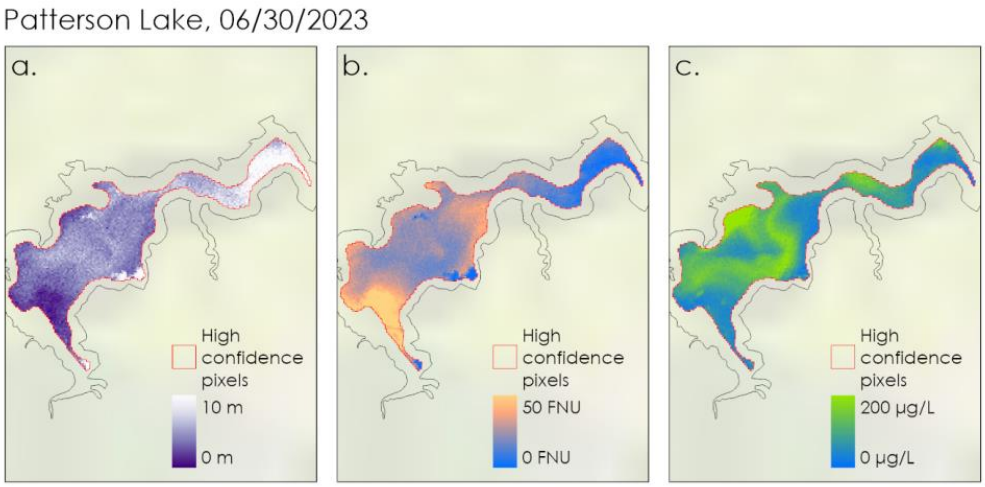

Figure 10. Three-panel map of Secchi depth (a), turbidity (b), and chlorophyll-a (c) concentrations in Patterson Lake on 30th June 2023

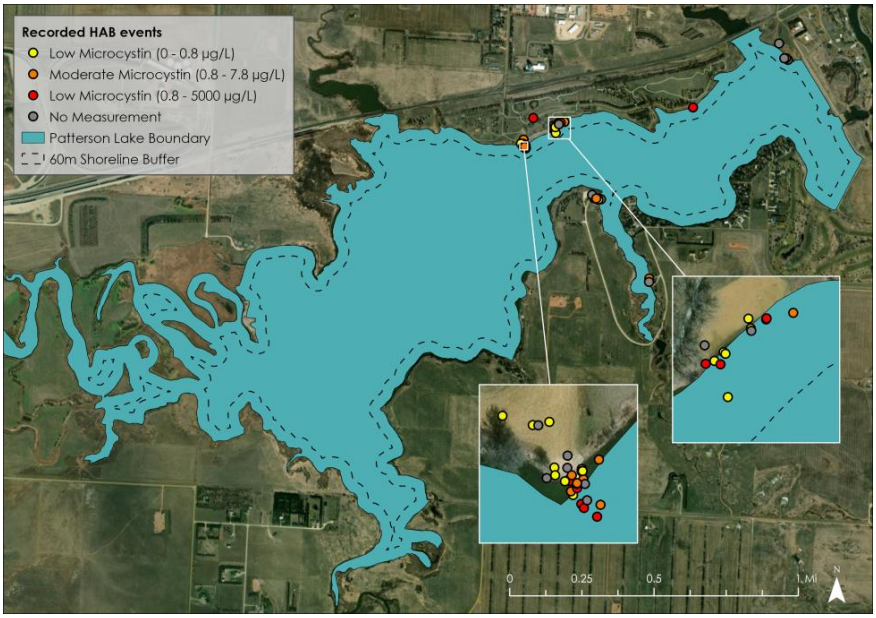

Figure 11. Map of recorded in situ HAB events in Patterson Lake (2020-2024)

The map of recorded in situ HAB events displays locations of high HAB activity in Patterson Lake, based on ND DEQ sampling efforts. These mostly occur near docks and boat ramps on the northern shoreline. The ND DEQ obtains in situ HAB microcystin concentrations via the ELISA method. HAB reports without a measurement are mapped, and the data are binned into quantiles. It should be noted that all sampling points fall outside of the 60m lake buffer used for LWQI extraction.

3.2 Errors & Uncertainties

Beyond the filtering methods applied to the Earth observation data, the remaining cloud cover still restricted image analysis. This occurred when cloud cover obstructed critical lake sections and potentially obscured the

data, producing incomplete images. The long and narrow geometry of Lake Ashtabula and Jamestown Reservoir resulted in fewer pixels representing the waterbody, increasing the occurrence of adjacency effect errors from surrounding land. Thus, quality control flagging removed a larger portion of available pixels. This reduced the amount of suitable data for generating HAB case study maps. Additionally, the lack of the red-edge band on Landsat sensors limited our use of Landsat imagery for chlorophyll-a data retrieval and analysis. This decreased the overall amount of remotely sensed chlorophyll-a data available for our analysis.

The in situ sampling data utilized in this project were limited by the availability of measurements taken by the ND DEQ Division of Water Quality, which reduced the overall amount of data for validation and comparison. In addition, the notable HAB observation datasheet did not always correspond to the exact day the HAB occurred and was reported (e.g. the actual HAB sample was collected a day after the HAB was reported). Finally, many of the in situ samples were taken on the outer edge of the lake. This is the portion of the lake that produces the highest source of remote sensing errors due to the adjacency effect, thus potentially compromising the accuracy of remotely sensed data.

LakeSense is currently a novel, unpublished workflow that has not been previously tested in North Dakota. This has led to gaps within the workflow that require additional troubleshooting. During the filtering process, various atmospheric corrections failed for certain satellite images depending on the pixel quality and cloud cover, which resulted in lower data availability for several atmospheric correction algorithms. The largest setback of using the LakeSense pipeline is its limited ability to distinguish between lakes and rivers. Due to the narrow and elongated shape of many lakes across North Dakota, the pipeline misidentified many of them as rivers and incorrectly excluded them from analysis.

4. Conclusions

4.1 Interpretation of Results

Analyses of Devils Lake and Patterson Lake revealed seasonal dynamics and interannual trends in lake water quality that are also evident in the three additional case study lakes (Appendix A-C). Across all sites, remote sensing data showed peaks in chlorophyll-a concentrations during the summer months of July and August, alongside dips in Secchi depth and, in certain years, increases in turbidity. These seasonal patterns are consistent with environmental drivers of HAB development, including higher temperatures and nutrient availability. In multiple lakes, chlorophyll-a peaks corresponded with in situ HAB sampling events, thus demonstrating that the LakeSense pipeline can detect conditions associated with confirmed HAB occurrences.

Interannual patterns revealed lake-specific dynamics with implications for targeted management. Patterson Lake exhibited a gradual increase in average turbidity and a corresponding decline in Secchi depth over the study period, indicating a long-term decline in water clarity. In contrast, Devils Lake results showed high chlorophyll-a variability but more stable turbidity and Secchi depth values. We observed similar lake-specific differences in the appendix lakes. These contrasts highlight the need for tailored monitoring strategies.

Despite limitations in spatial resolution and sensor band availability, the consistency of seasonal and multi-year variability across lake results supports the feasibility of using LakeSense to supplement ND DEQ's in situ monitoring. This approach can help prioritize sampling periods of elevated chlorophyll-a concentrations and reduced water clarity to optimize field sampling efforts under staff and budget constraints for lakes with known HAB risk. Long-term remote sensing data can provide early indicators of shifts in baseline LWQI conditions, and this may help partners improve management responses to HAB events.

4.2 Feasibility & Partner Implementation

Our findings assessed the feasibility of using Earth observation data within the LakeSense pipeline to analyze and monitor chlorophyll-a, Secchi depth, and turbidity across North Dakota. Sentinel-2 MSI, Landsat 8 OLI, and Landsat 9 OLI-2 imagery obtained through LakeSense enabled us to capture both seasonal dynamics and

multi-year trends in LWQI. Consistent variability patterns across these products complement in situ observations to increase the temporal and spatial coverage of LWQI data for HAB monitoring. We suggest ND DEQ Department of Water Quality continue in situ sampling efforts at sites highlighted by LakeSense analysis. Analyzing seasonal and interannual trends will allow them to be more selective with resource-intensive sampling efforts to enable streamlined HAB monitoring of North Dakota's lakes.

6. Acknowledgements

DEVELOP Lead – Madison Arndt; Science Advisors - Cédric Fichot & Sachini Ranasinghe (Boston University); Project Partners - Brian Houle & Joshua Wert (ND DEQ, Division of Water Quality); and DEVELOP Project Coordination Fellow – Isabel Tate

This material contains modified Copernicus Sentinel data (2015-2023), processed by ESA.

Any opinions, findings, and conclusions or recommendations expressed in this material are those of the author(s) and do not necessarily reflect the views of the National Aeronautics and Space Administration.

This material is based upon work supported by NASA through contract 80LARC23FA024.

6. Glossary

Adjacency effect – Excess scattering over the target water body, caused by high reflectance from surrounding bright land surfaces
AC – Atmospheric Correction
CDSE – Copernicus Data Space Ecosystem
K_d - Diffuse Attenuation Coefficient; Measure of changes in light attenuation with depth
Earth observations – Satellites and sensors that collect information about the Earth's physical, chemical, and biological systems over space and time
Eutrophic – Nutrient rich water within a lake
EXP – ACOLITE Exponential Extrapolation
GAAC – Genetic Algorithm for Atmospheric Correction
HAB – Harmful Algal Bloom
LWQI – Lake Water Quality Indicators
MET – Meteorological Satellites
MSI – MultiSpectral Instrument
ND DEQ – North Dakota Department of Environmental Quality
NHD ID – National Hydrography Dataset Identification
NIR – Near Infrared
OLI – Operational Land Imager
POI – Pole of Inaccessibility; The point within a lake that is the furthest possible distance from the shoreline boundaries
R_{rs} - Remote-sensing Reflectance; Ratio of water-leaving radiance to downwelling irradiance just above the water surface
QWIP – Quality Water Index Polynomial; Analyzes the reliability of lake water of lake water reflectance by evaluating the quality of data based on the spectral shape of the lake reflectance
USGS – United States Geological Survey
WQP –Water Quality Portal

7. References

Bramich, J., Bolch, C. J. S., & Fischer, A. (2021). Improved red-edge chlorophyll-a detection for Sentinel-2. *Ecological Indicators*, *120*, 106876. https://doi.org/10.1016/j.ecolind.2020.106876

Castagna, A., & Vanhellemont, Q. (2025). A generalized physics-based correction for adjacency effects. *Applied Optics*, *64*(10), 2719. https://doi.org/10.1364/ao.546766

Chen, L., Liu, L., Liu, S., Shi, Z., & Shi, C. (2025). The application of remote sensing technology in inland water quality monitoring and water environment science: Recent progress and perspectives. *Remote Sensing*, *17*(4), 667. https://doi.org/10.3390/rs17040667

Copernicus Sentinel-2 (processed by ESA). (2021). *MSI Level-2A BOA Reflectance Product. Collection 1. European Space Agency*. https://doi.org/10.5270/S2_-znk9xsj

Copernicus Sentinel-2 (processed by ESA). (2021). *MSI Level-1C TOA Reflectance Product. Collection 1. European Space Agency*. https://doi.org/10.5270/S2_-742ikth

Dierssen, H. M., Vandermeulen, R. A., Barnes, B. B., Castagna, A., Knaeps, E., & Vanhellemont, Q. (2022). QWIP: A quantitative metric for quality control of aquatic reflectance spectral shape using the apparent visible wavelength. *Frontiers in Remote Sensing*, *3*. https://doi.org/10.3389/frsen.2022.869611

Earth Resources Observation and Science (EROS) Center. (2020). Landsat 8-9 Operational Land Imager / Thermal Infrared Sensor Level-1, Collection 2 [dataset]. U.S. Geological Survey. https://doi.org/10.5066/P975CC9B

Earth Resources Observation and Science (EROS) Center. (2020). Landsat 8-9 Operational Land Imager / Thermal Infrared Sensor Level-2, Collection 2 [dataset]. U.S. Geological Survey. https://doi.org/10.5066/P9OGBGM6

Gons, H. J. (2002). A chlorophyll-retrieval algorithm for satellite imagery (medium resolution imaging spectrometer) of inland and coastal waters. *Journal of Plankton Research*, *24*(9), 947–951. https://doi.org/10.1093/plankt/24.9.947

Jia, T., Zhang, Y., Weng, C., & Dong, R. (2022). Improving remote sensing retrieval of global ocean transparency with optical water classification. *Ecological Indicators*, *143*, 109359. https://doi.org/10.1016/j.ecolind.2022.109359

Karthick, M., Shanmugam, P., & He, X. (2024). Enhanced polymer atmospheric correction algorithm for water-leaving radiance retrievals from hyperspectral/multispectral remote sensing data in inland and coastal waters. *Optics Express*, *32*(5), 7659. https://doi.org/10.1364/oe.504088

Karimi, B., Hashemi, S. H., & Aghighi, H. (2024). Application of Landsat 8 and Sentinel-2 for retrieval of chlorophyll-a in a shallow freshwater lake. *Advances in Space Research,* 74(1), 117–129. https://doi.org/10.1016/j.asr.2024.03.056

Main-Knorn, M., Pflug, B., Louis, J., Debaecker, V., Muller-Wilm, U., Gascon, F. (2017). Sen2Cor for Sentinel-2. *Image and Signal Processing for Remote Sensing XXIII*, 10427. https://doi.org/10.1117/12.2278218

Kulkarni, A. (2011). Water quality retrieval from Landsat TM imagery. *Procedia Computer Science*, *6*, 475–480. https://doi.org/10.1016/j.procs.2011.08.088

Lee, Z., Hu, C., Shang, S., Du, K., Lewis, M., Arnone, R., & Brewin, R. (2013). Penetration of UV-visible solar radiation in the global oceans: Insights from ocean color remote sensing. *Journal of Geophysical Research: Oceans*, *118*(9), 4241–4255. https://doi.org/10.1002/jgrc.20308

Lee, Z., Shang, S., Hu, C., Du, K., Weidemann, A., Hou, W., Lin, J., & Lin, G. (2015). Secchi disk depth: A new theory and mechanistic model for underwater visibility. *Remote Sensing of Environment*, *169*, 139–149. https://doi.org/10.1016/j.rse.2015.08.002

Mishra, S., & Mishra, D. R. (2012). Normalized difference chlorophyll index: A novel model for remote estimation of chlorophyll-a concentration in turbid productive waters. *Remote Sensing of Environment*, *117*, 394–406. https://doi.org/10.1016/j.rse.2011.10.016

Nechad, B., Ruddick, K.G., Park, Y. (2010). Calibration and validation of a generic multisensor algorithm for mapping of total suspended matter in turbid waters. *Remote Sensing of Environment*, 114, 854-866. https://doi.org/10.1016/j.rse.2009.11.022.

Nolte, C., Fichot, C., Ranasinghe, S., Moore, C., Boyle, K., & Friedl, M. (2025). *Project: LakeSense.* https://placeslab.org/lakesense/

North Dakota Department of Health (2019). *North Dakota 2018 Integrated Section 305(b) Water Quality Assessment Report and Section 303(d) List of Waters Needing Total Maximum Daily Loads.* https://deq.nd.gov/publications/WQ/3_WM/TMDL/1_IntegratedReports/2018_Final_ND_Integrated_Report_20190426.pdf

Novoa, S., Doxaran, D., Ody, A., Vanhellemont, Q., Lafon, V., Lubac, B., & Gernez, P. (2017). Atmospheric corrections and multi-conditional algorithm for multi-sensor remote sensing of suspended particulate matter in low-to-high turbidity levels coastal waters. *Remote Sensing*, 9(1), 61. https://doi.org/10.3390/rs9010061

O'Reilly, J. E., & Werdell, P. J. (2019). Chlorophyll algorithms for ocean color sensors - OC4, OC5 & OC6. *Remote Sensing of Environment*, *229*, 32–47. https://doi.org/10.1016/j.rse.2019.04.021

Pahlevan, N., Schott, J. R., Franz, B. A., Zibordi, G., Markham, B., Bailey, S., Schaaf, C. B., Ondrusek, M., Greb, S., & Strait, C. M. (2017). Landsat 8 remote sensing reflectance (RRS) products: Evaluations, intercomparisons, and enhancements. *Remote Sensing of Environment*, *190*, 289–301. https://doi.org/10.1016/j.rse.2016.12.030

Pan, Y., & Bélanger, S. (2025). Genetic algorithm for Atmospheric Correction (GAAC) of water bodies impacted by adjacency effects. *Remote Sensing of Environment*, *317*, 114508. https://doi.org/10.1016/j.rse.2024.114508

Pitarch, J., & Vanhellemont, Q. (2021). The QAA-RGB: A universal three-band absorption and backscattering retrieval algorithm for high resolution satellite sensors. development and implementation in ACOLITE. *Remote Sensing of Environment*, *265*, 112667. https://doi.org/10.1016/j.rse.2021.112667

Sun, Y., Wang, D., Li, L., Ning, R., Yu, S., & Gao, N. (2024). Application of remote sensing technology in water quality monitoring: From traditional approaches to artificial intelligence. *Water Research*, 267, 122546. https://doi.org/10.1016/j.watres.2024.122546

Vermote, E., Justice, C., Claverie, M., Franch, B. (2016). Preliminary analysis of the performance of the Landsat 8/OLI land surface reflectance product, *Remote Sensing of Environment*, 185, 46-56. https://doi.org/10.1016/j.rse.2016.04.008

8. Appendices

Appendix A: Jamestown Reservoir

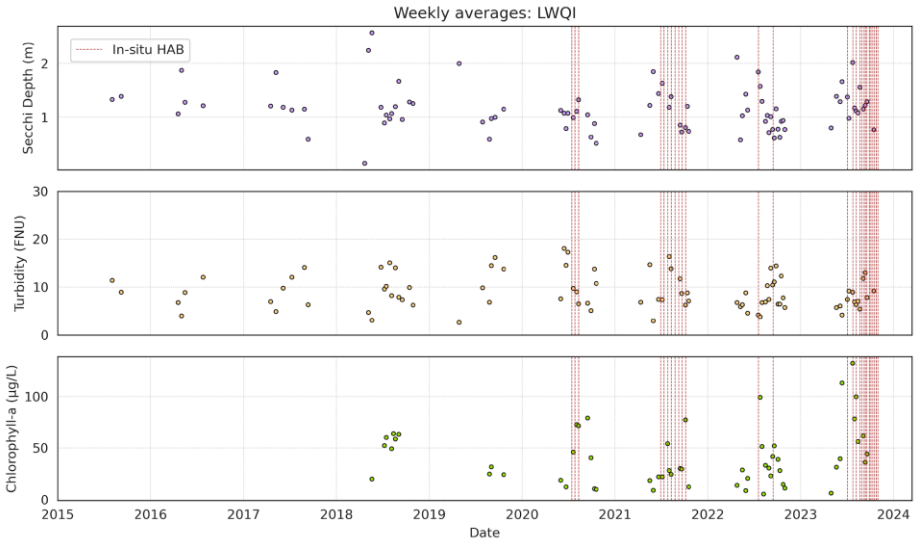

Figure A1. Time series of weekly average LWQI values across Jamestown Reservoir. Each time series plot represents monthly average Secchi depth, turbidity, and chlorophyll-a trends from 2015/2018 to 2023.

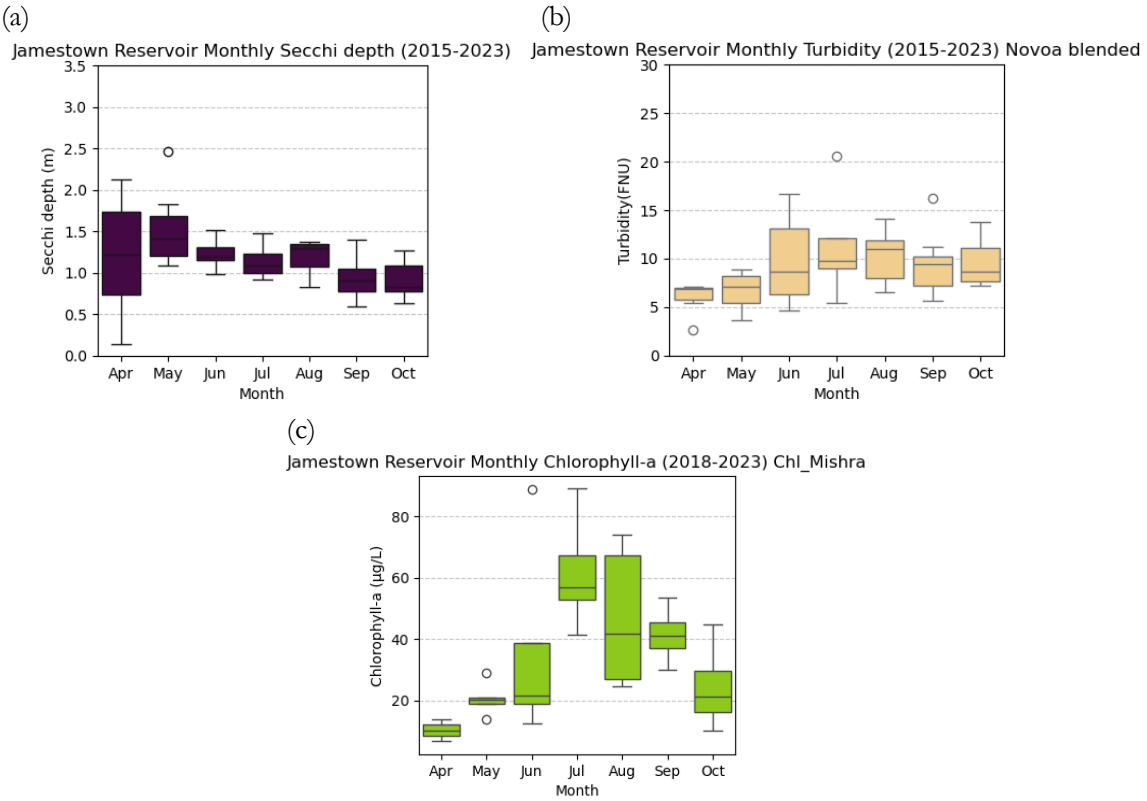

Figure A2. Seasonality boxplots of monthly average Secchi depth (a), turbidity (b), and chlorophyll-a (c) across Jamestown Reservoir from 2015/2018 to 2023

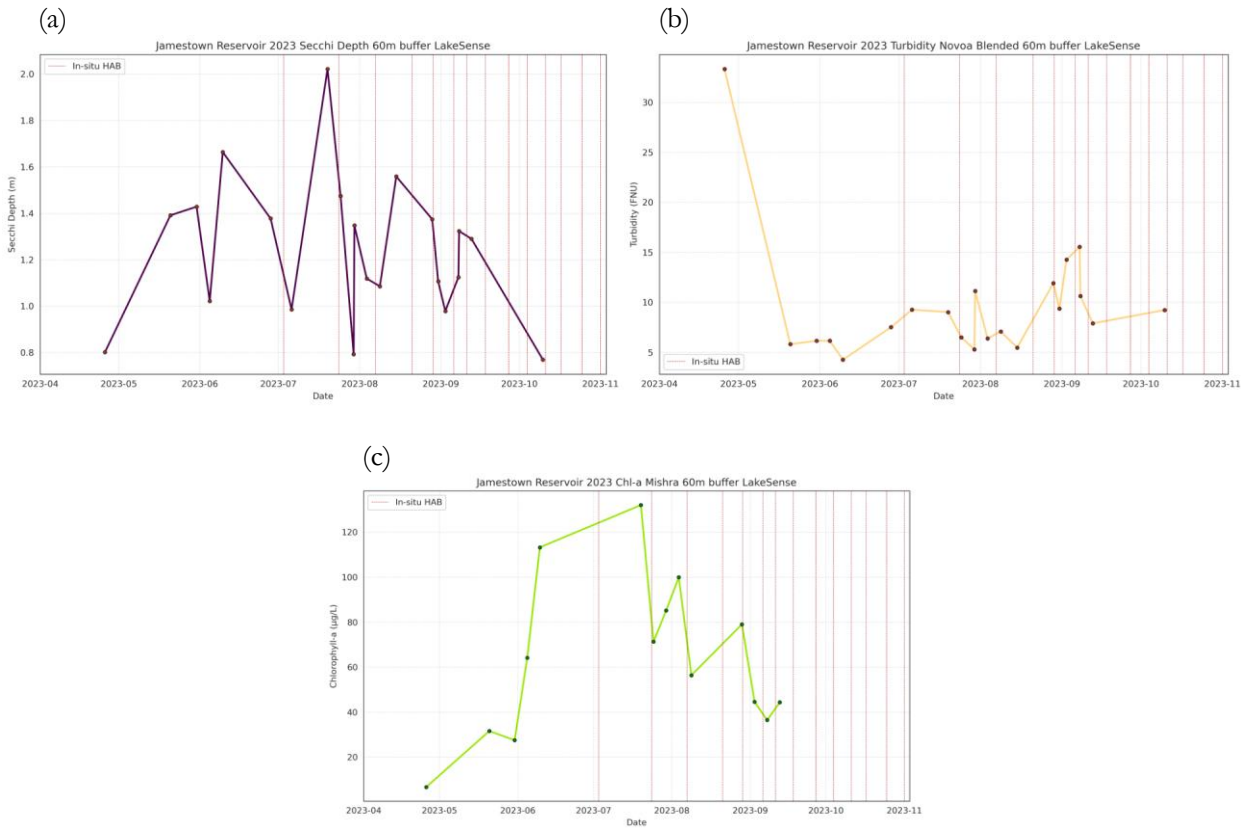

Figure A3. 2023 snapshots of monthly average Secchi depth (a), turbidity (b), and chlorophyll-a (c) across Jamestown Reservoir from April to November 2023

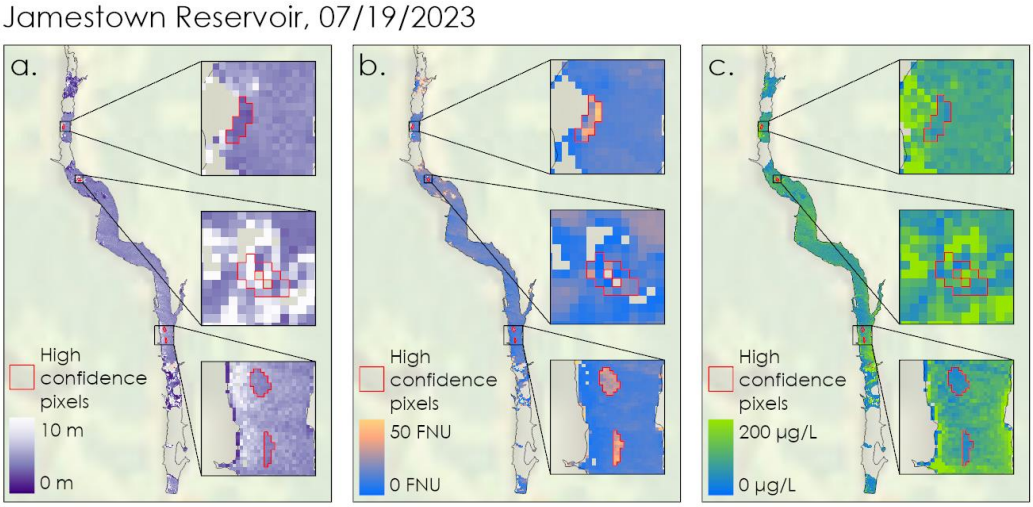

Figure A4. Three-panel map of Secchi depth (a), turbidity (b), and chlorophyll-a (c) concentrations in Jamestown Reservoir on 19h July 2023

Figure A5. Map of recorded in situ HAB events in Jamestown Reservoir (2020 - 2024)

Appendix B: Lake Ashtabula

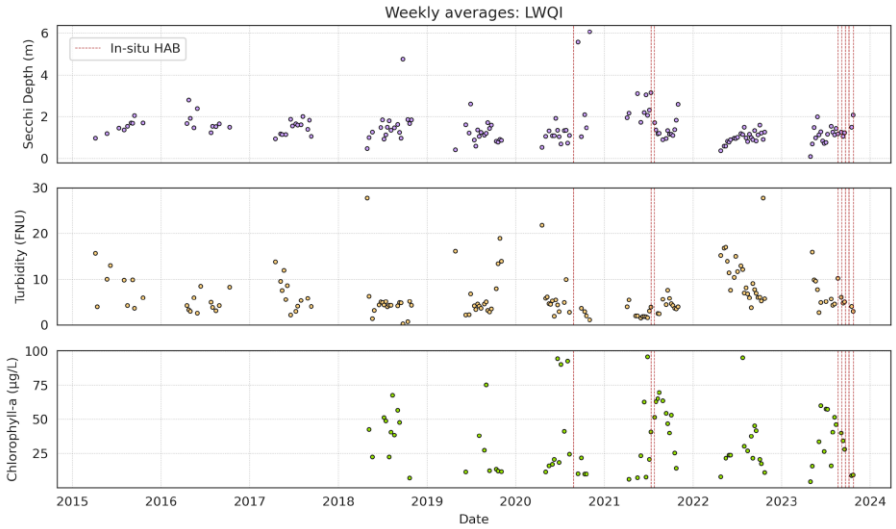

Figure B1. Time series of weekly average LWQI values across Lake Ashtabula. Each time series plot represents monthly average Secchi depth, turbidity, and chlorophyll-a trends from 2015/2018 to 2023.

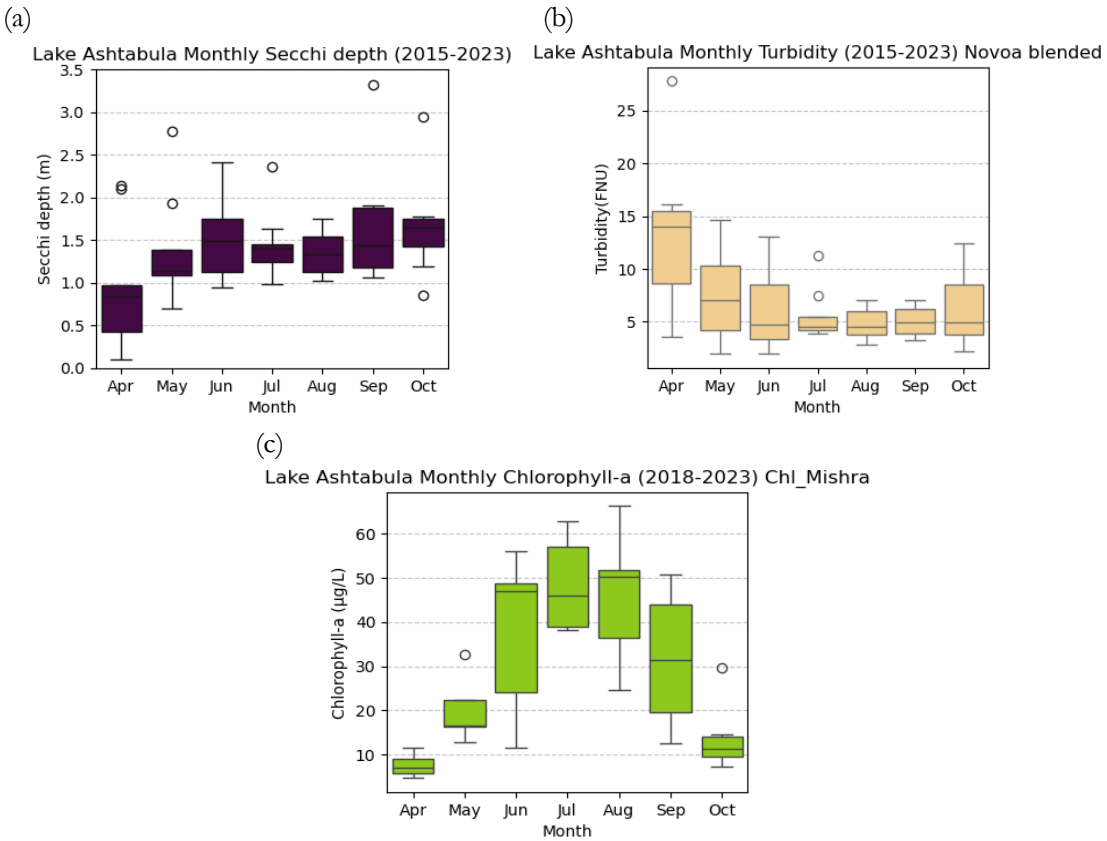

Figure B2. Seasonality boxplots of monthly average Secchi depth (a), turbidity (b), and chlorophyll-a (c) across Lake Ashtabula from 2015/2018 to 2023

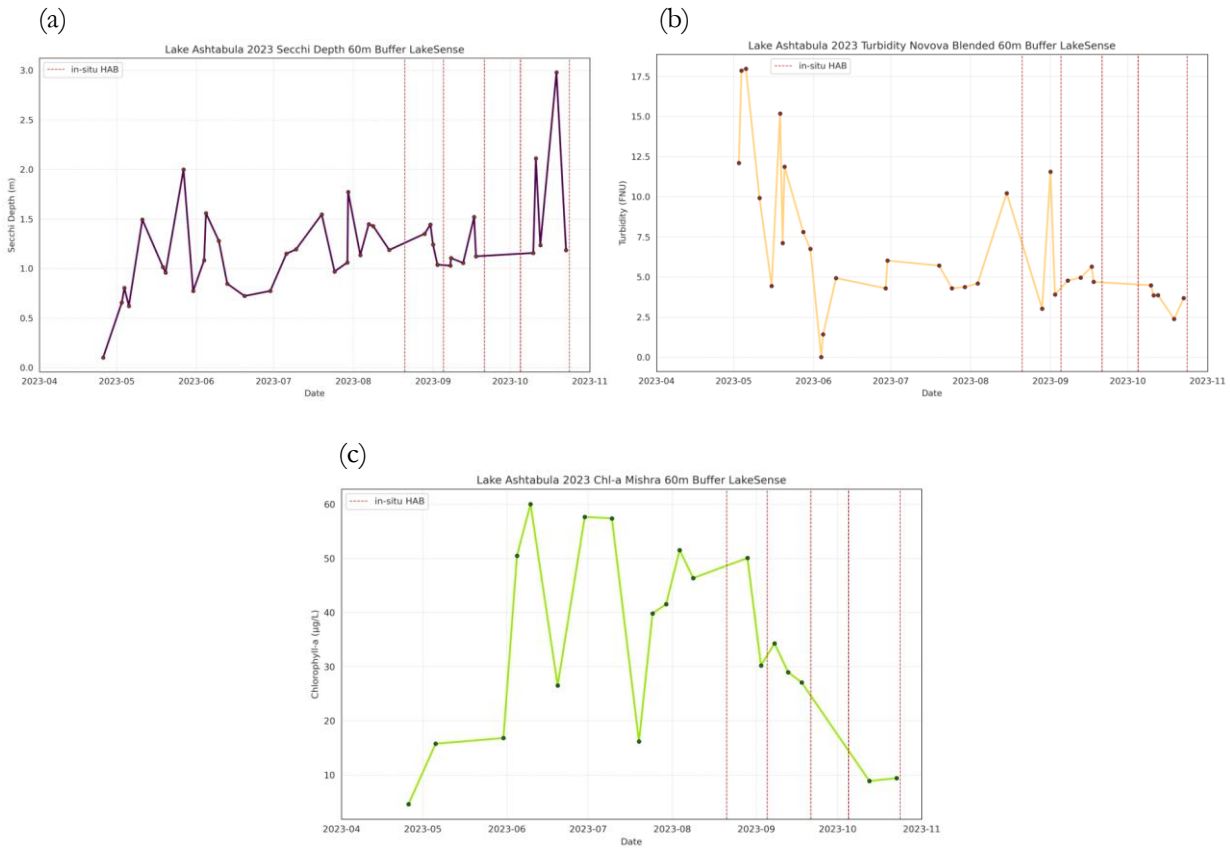

Figure B3. 2023 snapshots of monthly average Secchi depth (a), turbidity (b), and chlorophyll-a (c) across Lake Ashtabula from April to November 2023

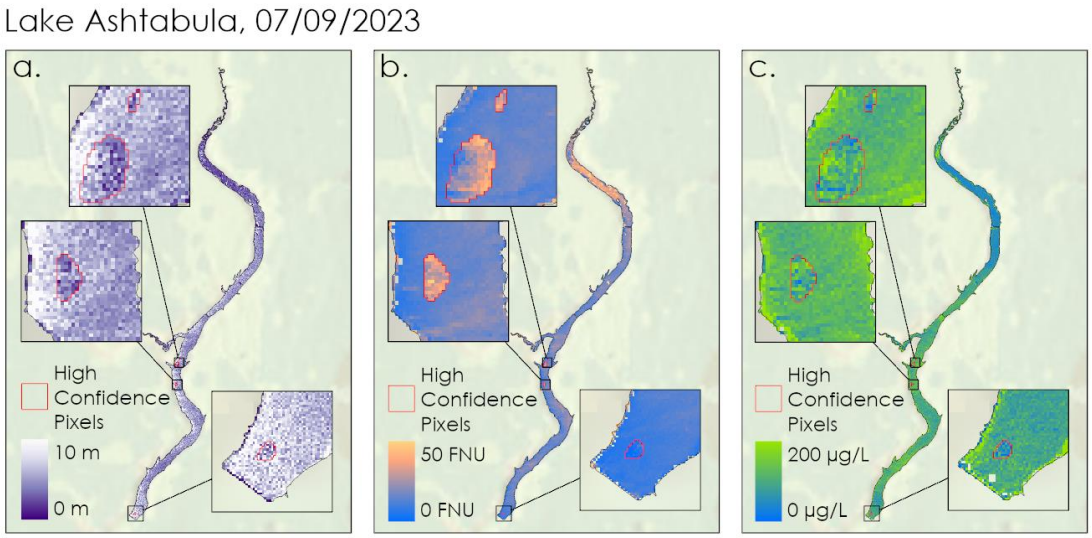

Figure B4. Three-panel map of Secchi depth (a), turbidity (b), and chlorophyll-a (c) concentrations in Lake Ashtabula on 9th July 2023

Figure B5. Map of recorded in situ HAB events in Lake Ashtabula (2020 - 2024)

Appendix C: Bowman-Haley Dam

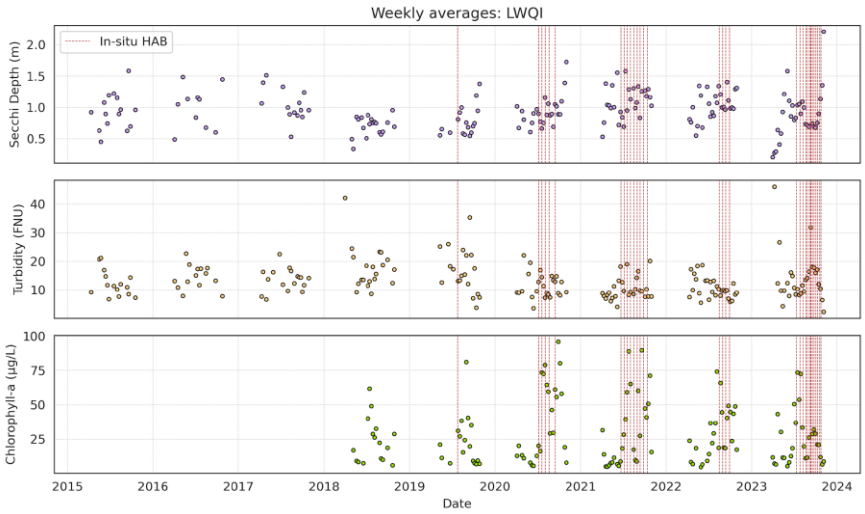

Figure C1. Time series of weekly average LWQI values across Bowman-Haley Dam. Each time series plot represents monthly average Secchi depth, turbidity, and chlorophyll-a trends from 2015/2018 to 2023.

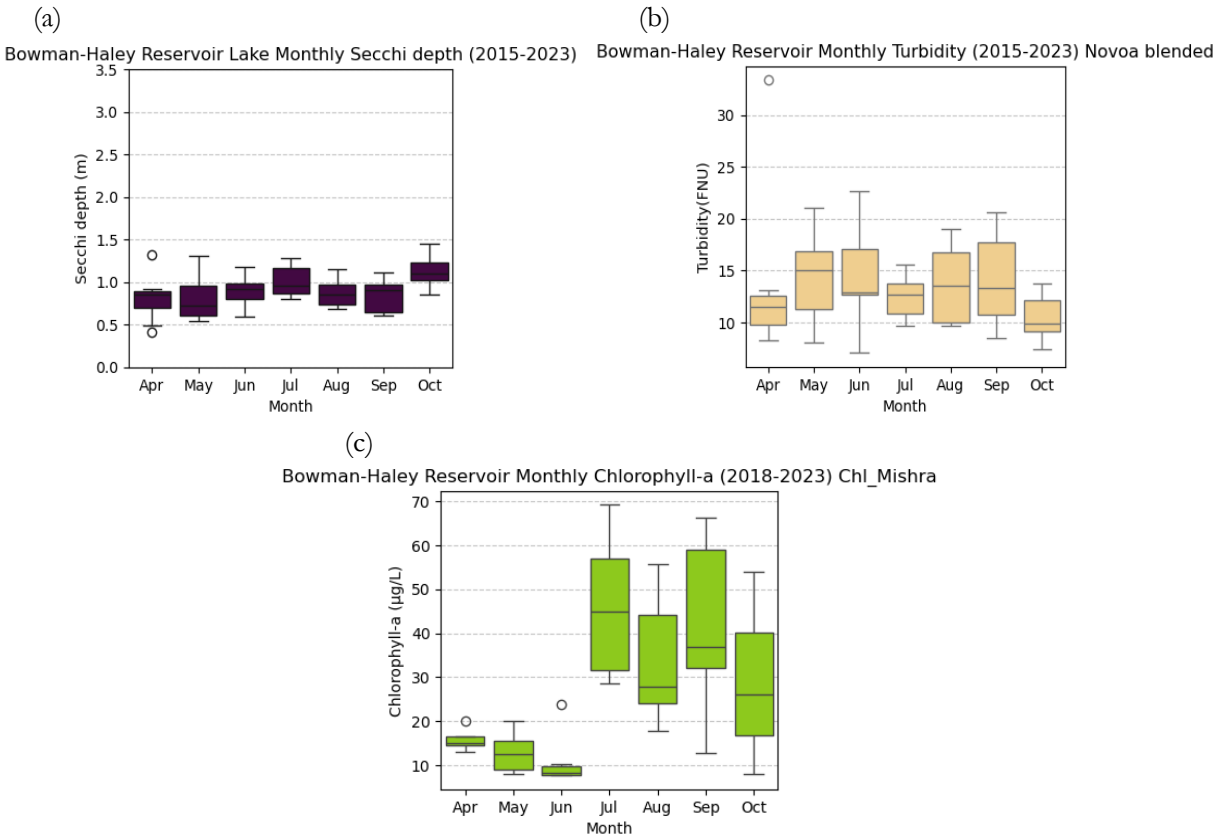

Figure C2. Seasonality boxplots of monthly average Secchi depth (a), turbidity (b), and chlorophyll-a (c) across Bowman-Haley from 2015/2018 to 2023

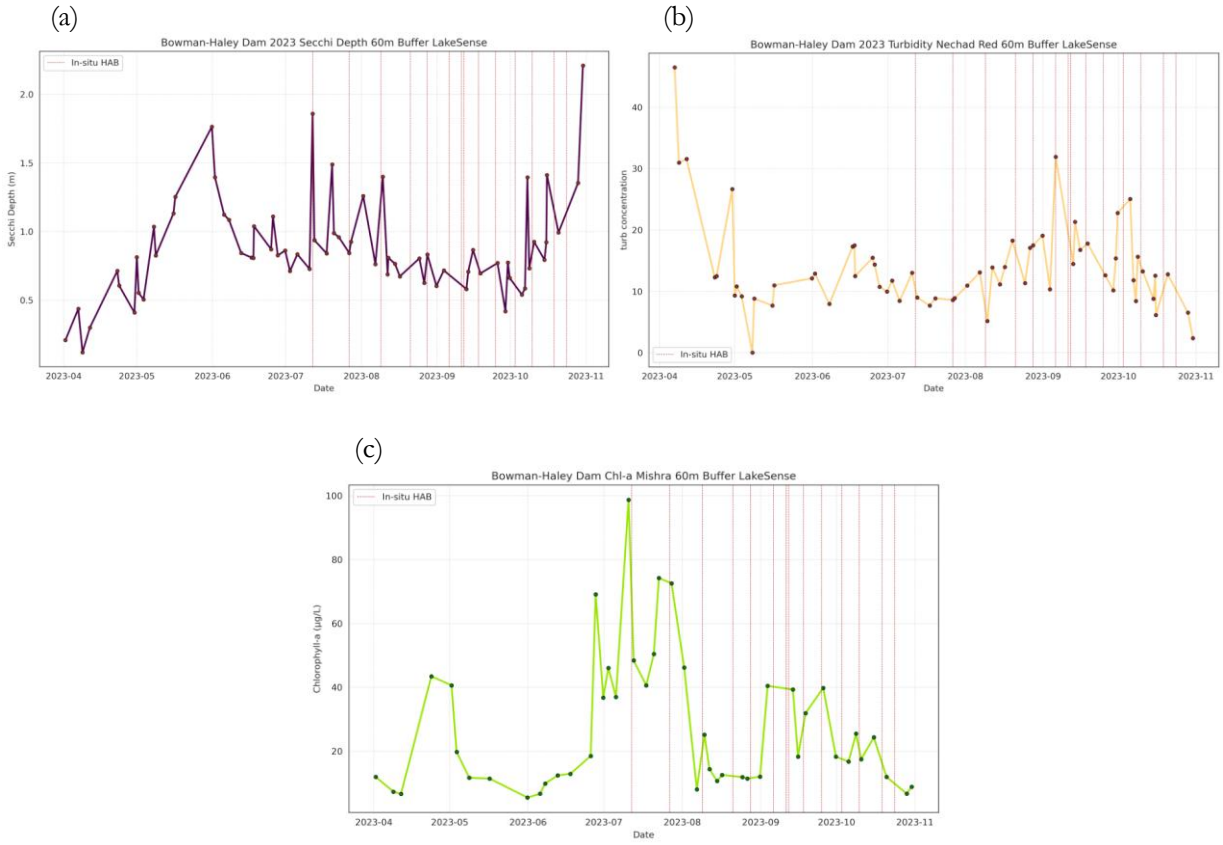

Figure C3. 2023 snapshots of monthly average Secchi depth (a), turbidity (b), and chlorophyll-a (c) across Bowman-Haley Dam from April to November 2023

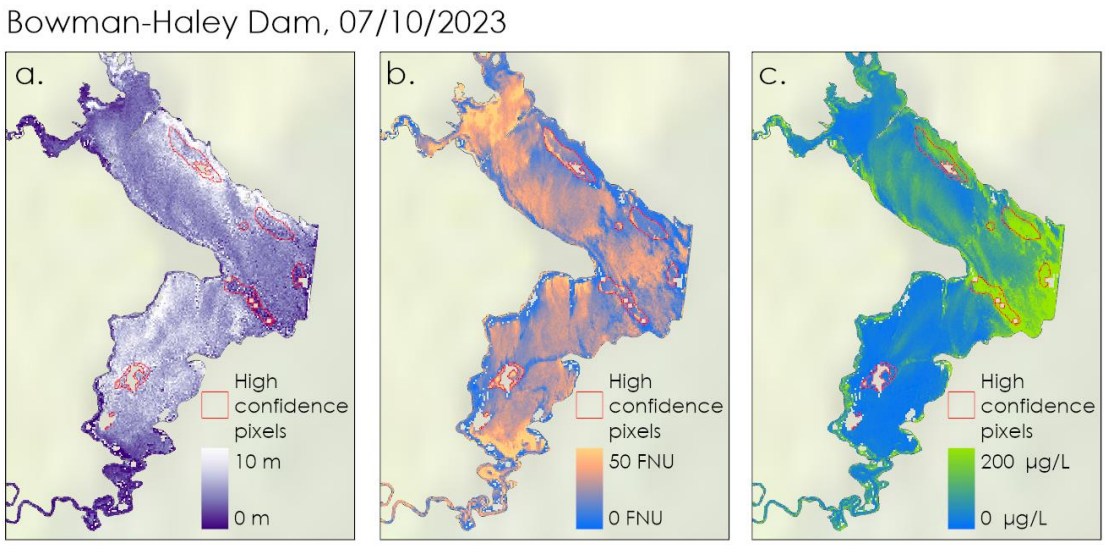

Figure C4. Three-panel map of Secchi depth (a), turbidity (b), and chlorophyll-a (c) concentrations in Bowman-Haley Dam on 10th July 2023

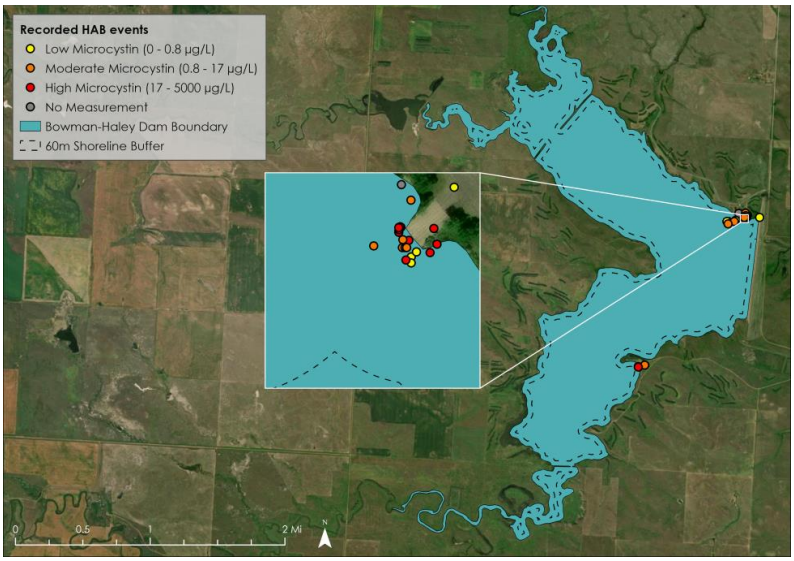

Figure C5. Map of recorded in situ HAB events in Bowman-Haley Dam (2020 - 2024)